

1 **Enhanced flow-motion complexity of skin microvascular perfusion in Sherpas and**  
2 **lowlanders during ascent to high altitude**

3 Deborah Carey<sup>1</sup>, Marjola Thanaj<sup>1</sup>, Thomas Davies<sup>2</sup>, Edward Gilbert-Kawai<sup>2</sup>, Kay Mitchell<sup>3,5,6</sup>,  
4 Denny Z. H. Levett<sup>3,5,6</sup>, Michael G. Mythen<sup>2</sup>, Daniel S. Martin<sup>2</sup>, Michael P. Grocott<sup>2,3,4,5,6</sup>,  
5 Andrew J. Chipperfield<sup>1</sup>, Geraldine F. Clough<sup>4</sup>

6

7 <sup>1</sup>Faculty of Engineering and Physical Sciences, University of Southampton, Southampton, UK.

8 <sup>2</sup>University College London Centre for Altitude Space and Extreme Environment Medicine, UCLH  
9 NIHR Biomedical Research Centre, Institute for Sports Exercise and Health, London, UK.

10 <sup>3</sup>Integrative Physiology and Critical Illness Group, Clinical and Experimental Sciences, Faculty of  
11 Medicine, University of Southampton, Southampton, UK.

12 <sup>4</sup>Faculty of Medicine, University of Southampton, Southampton, UK.

13 <sup>5</sup>Respiratory and Critical Care Research Theme, Southampton NIHR Biomedical Research Centre,  
14 University Hospital Southampton NHS Foundation Trust / University of Southampton.

15

16 <sup>6</sup>Anaesthesia and Critical Care Research Unit, University Hospital Southampton NHS Foundation  
17 Trust, Southampton, UK.

18

19

20 **CORRESPONDING AUTHOR**

21 Geraldine Clough BSc PhD

22 Emeritus Professor of Vascular Physiology

23 Institute of Developmental Sciences, Faculty of Medicine, University of Southampton,  
24 Southampton General Hospital (MP 887), Southampton, SO16 6YD, UK.

25 [g.f.clough@soton.ac.uk](mailto:g.f.clough@soton.ac.uk)

26

## 27 **ABSTRACT**

28 An increased and more effective microvascular perfusion is postulated to play a key role in  
29 the physiological adaptation of Sherpa highlanders to the hypobaric hypoxia encountered at  
30 high altitude. To investigate this, we used Lempel-Ziv complexity (LZC) analysis to explore  
31 the spatiotemporal dynamics of the variability of the skin microvascular blood flux (BF)  
32 signals measured at the forearm and finger, in 32 lowlanders (LL) and 46 Sherpa  
33 highlanders (SH) during the Xtreme Everest 2 expedition. Measurements were made at  
34 baseline (BL) (LL: London 35m; SH: Kathmandu 1300m) and at Everest base camp (LL and  
35 SH: EBC 5,300m). We found that BF signal content increased with ascent to EBC in both  
36 SH and LL. At both altitudes, LZC of the BF signals was significantly higher in SH, and was  
37 related to local slow-wave flow-motion activity over multiple spatial and temporal scales. In  
38 SH, BF LZC was also positively associated with LZC of the simultaneously measured tissue  
39 oxygenation signals. These data provide robust mechanistic information of microvascular  
40 network functionality and flexibility during hypoxic exposure on ascent to high altitude. They  
41 demonstrate the importance of a sustained heterogeneity of network perfusion, associated  
42 with local vaso-control mechanisms, to effective tissue oxygenation during hypobaric  
43 hypoxia.

44

45

## 46 **INTRODUCTION**

47

48 Sherpas highlanders (SH) are known to demonstrate considerable tolerance to hypobaric  
49 hypoxia, however, the mechanisms behind this adaptation are not well understood<sup>1</sup>.  
50 Previous studies have shown that SH exhibit a lower arterial oxygen content than lowlanders  
51 (LL) who ascend to comparable altitudes<sup>2-4</sup>, and thus it has been suggested that the  
52 mechanisms that facilitate SH apparent hypoxia tolerance reside, in part, within the  
53 microcirculation<sup>5-8</sup>. Adaptive SH microcirculatory mechanisms that are not evident in LL  
54 include a sustained microvascular perfusion and dilator capacity measured in the skin<sup>8,9</sup> and  
55 a higher microvascular flow index (MFI) and reduced perfusion heterogeneity index (HI) in  
56 the small (<25  $\mu$ m) vessels of the sublingual mucosa<sup>7,8</sup>.

57

58 Blood flow within a microcirculatory network is highly variable and its distribution and  
59 magnitude determined by local and regional metabolic demand. Local control of blood flow  
60 ensures matching of perfusion to spatially varying oxygen demand, thereby achieving  
61 efficient oxygen delivery<sup>10,11</sup>. Regulation of microvascular perfusion is predominately

62 achieved through changes in network conductance, modulated at a local level by  
63 endothelial, neurogenic, and myogenic regulatory activity<sup>12</sup>. Together, these activities  
64 determine the cyclic oscillations of arteriolar diameter (vasomotion) that are related to  
65 changes in blood flow distribution in the microvascular networks (flow-motion)<sup>13</sup>. The relative  
66 contribution of this rhythmic, low frequency oscillatory activity, as well as higher frequency  
67 cardiac and respiratory rhythms to microvascular perfusion has been assessed using  
68 spectral analysis of blood flux (BF) signals obtained using non-invasive laser Doppler  
69 fluximetry in the skin<sup>14</sup>. This has led to the suggestion that measurement of flow-motion  
70 activity may provide an early indicator of declining function (for review see<sup>53</sup>). In SH, the  
71 sustained network perfusion seen on exposure to hypobaric hypoxia has been associated  
72 with an enhanced low frequency flow-motion activity that was not evident in LL<sup>8,9</sup>. However,  
73 the extent to which such changes in local low-frequency oscillatory activity contributes to the  
74 observed variability in microvascular blood flow under conditions of hypobaric hypoxia<sup>7,8</sup>  
75 remains unexplored; as does the extent to which such oscillatory activity may be beneficial  
76 to tissue oxygenation under such conditions<sup>11,16,17</sup>.

77

78 Nonlinear complexity measures have been extensively used to assess the variability or loss  
79 of randomness of bio-signals notably electroencephalograms<sup>18</sup> and electrocardiograms<sup>19</sup>.  
80 The spatiotemporal variability of these signals reflect the physiological adaptability of the  
81 system and are established biomarkers of overall health status<sup>20</sup>. We and others have used  
82 non-linear analysis, such as Lempel-Ziv (LZ) complexity<sup>21</sup>, to determine the information  
83 content of microcirculatory blood flow signals as a metric of perfusion variability<sup>22,23</sup>. To  
84 date, these measures have confirmed a declining regularity and randomness of  
85 microcirculatory BF signals in both a primate model of diabetes<sup>25</sup> and in humans with or at  
86 risk of cardiovascular disease (CVD) in whom microvascular dysfunction is evident<sup>26</sup>. To  
87 what extent the variability in the BF signals arising from the cumulative activity (and temporal  
88 variation) of all the processes modulating microvascular blood flow differs between SH and  
89 LL, and with ascent to altitude, has yet to be explored; as does the impact of the complexity  
90 of the BF signal on effective tissue oxygenation.

91

92 The processes that regulate the cardiovascular system operate across multiple temporal  
93 scales. Consequently, multiscale nonlinear analysis of complex oscillatory signals such as  
94 heart rate variability has been used, in addition to traditional time- and frequency-domain  
95 analysis, as a tool to enhance diagnosis and risk stratification<sup>26</sup>. The rhythmical oscillatory  
96 processes that determine flow-motion, and that operate across differing time-scales in the  
97 range ~0.6-100 seconds, have similarly been explored using multiscale non-linear analysis  
98 of the laser Doppler BF signal<sup>22,23,27</sup>. To date these studies have shown multiscale

99 complexity analysis to be a good predictor of the variability of the signal over multiple time  
100 scales<sup>22,23,27</sup> and that they may provide novel mechanistic insight into the extent to which the  
101 BF signal is modulated by the different frequency bands under differing (patho)physiological  
102 conditions<sup>24,25</sup>.

103

104 The primary objective of the current study was to investigate the complexity of the oscillatory  
105 rhythms in microvascular blood flow and tissue oxygenation signals obtained in the skin of  
106 individuals ascending to 5300m as participants of the XE2 research expedition<sup>28</sup>, using non-  
107 linear uni- and multi-scale approaches. We hypothesised that non-linear approaches will  
108 provide novel information on the processes by which SH preserve superior peripheral  
109 microcirculatory perfusion at altitude<sup>7-9</sup>. We also sought to explore whether an enhanced  
110 complexity of the BF signal was associated with the more efficient oxygen delivery  
111 postulated to play a key role in the physiological adaptation of Sherpas to hypobaric  
112 hypoxia<sup>5-8</sup>.

113

114 Microvascular blood flux was measured non-invasively using laser Doppler fluximetry at two  
115 skin sites; that of the well characterised ventral forearm under both endothelium dependent  
116 and neurovascular control, and that of the finger pulp in which BF is largely determined by  
117 the abundantly present arteriovenous anastomoses under sympathetically mediated  
118 constrictor tone<sup>29</sup>. The analysis of signals from both beds allowed us to explore the  
119 differential impact of local flow-motion activity on the complexity of microvascular perfusion.

120

121

## 122 **MATERIALS AND METHODS**

### 123 ***Study Participants***

124 The signals analysed are from measurements made in 32 lowlanders (LL) all of whom were  
125 born and lived below 1000m, and were not from a native high altitude population, and 46  
126 Sherpa highlanders (SH). These 78 individuals represent a subset of the 144 participants of  
127 the Xtreme Everest 2 research expedition (XE2)<sup>28</sup> in whom we have previously reported the  
128 effects of hypobaric hypoxia on microvascular blood flow in the time and spectral domains<sup>7</sup>.  
129 Approval of the study design, risk management plan and protocol were obtained from both  
130 the University College London Research Ethics Committee (Ref: 3750/002) and the Nepal  
131 Health Research Council (NHRC) (1334). The study was performed to the standards set by  
132 the Declaration of Helsinki, except for registration in a database. All participants provided  
133 written informed consent for participation in the studies.

134

**135 Tissue Blood Flux and Oxygenation Signal Capture**

136 Skin microvascular blood flux (BF) and tissue oxygenation (OXY) signals, and skin  
137 temperature were recorded simultaneously at the forearm using a combined laser Doppler  
138 fluximetry (LDF) and white light reflectance spectroscopy probe (CP1T-1000  
139 LDF™/OXY™/temperature probe, Moor Instruments Ltd, Axminster, UK) placed  
140 approximately 10 cm proximal to the wrist. A second combined LDF™/temperature probe  
141 (VP1T, Moor, Axminster, UK) was placed on the pulp of the index finger. Probe position was  
142 recorded with a photograph and permanent marker pen to ensure use of the same  
143 anatomical site in subsequent measurements as previously described<sup>7</sup>.

144 Signals were collected at baseline (BL) in London for LL (35m), and in Kathmandu (1300m)  
145 for SH, and at Everest Base Camp (EBC) (5300m) as described previously<sup>8</sup>. Measurements  
146 were made on the morning of day 2 after arrival at EBC after an 11 day trek from Lukla  
147 (2800m). Participants lay in a supine position during signal capture with their non-dominant  
148 arm resting at heart level. Full details of the environmental and physiological measurements  
149 made at each altitude are given elsewhere<sup>7</sup>.

150

**151 Signal Analysis**

152 All signals were captured at a 40Hz sampling rate using the manufacturer's software  
153 (moorVMS-PC software, Moor Instruments Ltd, Axminster, UK) and a continuous 10 min  
154 sample of each signal extracted for analysis in the time and spectral domain. The signals  
155 analysed were resting skin blood flux (BF, in arbitrary perfusion units, PU) and oxygenated  
156 Hb (oxyHb, in arbitrary units, AU). We elected to focus on the oxyHb output as the prime  
157 tissue oxygenation signal for the complexity analysis as suggested by our previous studies<sup>22</sup>.

158 The complexity of the BF and oxyHb signals arising from rhythmical flow-motion activity was  
159 explored using non-linear LZ complexity (LZC) analysis<sup>21</sup> to determine how much the BF and  
160 oxyHb signals differed from a random sequence of finite symbolic sequences derived from  
161 the time series<sup>20,30</sup>. The signals were represented as a binary string using delta encoding  
162 whereby a zero is recorded if a value is less than the previous value in the time series and a  
163 one when it is greater than that previously<sup>22,23</sup>. The LZC is a measure of the information  
164 content, or effort to describe, a signal and is the length of the shortest instruction set  
165 required to reconstruct it without loss of information. A random signal would have high  
166 complexity as there are no rules that define it whereas a periodic signal would have low  
167 complexity as the same terms are repeated continually. LZC analysis does not require the

168 signal to be strongly stationary, unlike chaos-based entropy analysis and thus the signal can  
169 be normalised to the length of the sample window<sup>31</sup>. Exhaustive LZC, where the signal is  
170 decomposed into all the instructions required to reproduce it, was then calculated for each  
171 40 second epoch to determine the complexity lower bound. A complexity index (LZC index)  
172 was calculated as the mean of the 15 × 40 second epochs for each sampled signal to  
173 provide an index of the dynamic activity modulating the BF and oxyHb signals.

174 The physiological processes that modulate flow-motion and determine the information  
175 content of the BF signals operate at frequencies ranging from 0.001Hz to 2Hz<sup>14</sup>. They also  
176 appear to vary with altitude<sup>8,9</sup>. To take account of these multiple, and potentially varying,  
177 process scales we measured LZC in multiple time-scales (MLZC) using a coarse-graining  
178 approach<sup>25,32,45</sup>. MLZC was explored between scales  $\tau = 1-12$ , as the maximum frequency of  
179 interest is governed by an upper limit of heart rate of 1.6 Hz and Nyquist frequency twice this  
180 or 3.2 Hz which corresponds to scale  $\tau = 12$ . To determine the association between the  
181 complexity of the BF signal and the mechanisms underlying flow-motion we calculated the  
182 Spearman correlations for relative power spectral density of the endothelial (0.0095-0.02  
183 Hz), sympathetic (0.02-0.06 Hz), myogenic (0.06-0.15 Hz), respiratory (0.15-0.4 Hz), and  
184 cardiac (0.4-1.6 Hz)<sup>14</sup> spectral bands and LZC measured at each time scale (MLZC).

185

## 186 **Statistical Analysis**

187 Statistical analyses were performed using SPSS for Windows version 25.0 (IBM, USA). Data  
188 were tested for Gaussian distribution using the Kolmogorov-Smirnov test and visual  
189 inspection of histograms. As the BF signal data did not show a normal distribution, data are  
190 presented as median (95%CI). SH and LL cohorts at BL and EBC were compared using two-  
191 way ANOVA. We used Mann Whitney U test and Wilcoxon Signed Rank test to compare  
192 single cohorts between BL and EBC. The relationships between BF, oxyHb and network  
193 perfusion complexity at each site were assessed individually using Spearman's rank  
194 correlation coefficient. A p-value of <0.05 was considered statistically significant for all  
195 analyses. We used multivariable linear regression models to explore factors that were  
196 independently associated, with microvascular network perfusion heterogeneity and  
197 oxygenation as the dependent (outcome) variables. Explanatory variables included in the  
198 models were skin temperature, age and gender, with site included as a binary indicator  
199 variable.

200

201

## 202 **RESULTS**

203

204 Artefact-free skin BF and tissue oxygenation signals (**Fig 1**) of sufficient length for LZC  
205 analysis at both BL and EBC, were obtained in 32 LL (16M/16F), age 46(14)y, BMI 24.3(3.3)  
206 kg/m<sup>2</sup> (mean(SD)) and 46 SH (23M/23F), age 28(6)y (p=0.0001, SH vs LL) and BMI  
207 23.8(3.4) kg/m<sup>2</sup> (p>0.05, SH vs LL) who represented a subset of the 144 participants from  
208 the Xtreme Everest 2 research expedition (XE2)<sup>28</sup>.

209 The time domain characteristics of microcirculatory BF signals from the current subset of  
210 XE2 individuals used for complexity analysis are summarised in **Table 1**. Resting skin BF  
211 (PU) at the forearm of the 46 SH decreased with ascent to EBC, while that of the 32 LL  
212 remained unchanged, as reported previously in the full cohort<sup>8</sup>. In both sub-groups, resting  
213 BF at the finger decreased on ascent to EBC compared to BL (both p<0.001). Skin  
214 temperature varied between groups and with ascent to EBC but was notably higher at the  
215 finger in SH at both BL and EBC (Table 1). In both groups resting BF were positively  
216 associated with skin temperature at BL at the forearm (LL, r= 0.370 p=0.037; SH, r= 0.577  
217 p<0.0001) and at the finger (LL, r= 0.436 p=0.013; SH, r=0.764 p<0.0001). This association  
218 was lost at EBC in LL (p>0.05 for forearm and finger), but not in SH (forearm r=0.261  
219 p=0.021; finger r=0.643 p>0.0001).

220 Peripheral oxygen saturation (SpO<sub>2</sub>) declined with ascent to EBC in both LL and SH  
221 (p<0.001), as did tissue oxygenation (StO<sub>2</sub>) measured at the forearm using VMISOXY  
222 (p<0.001)<sup>8</sup>.

223

### 224 ***LZ complexity of microcirculatory blood flux and oxygenation signals increases with*** 225 ***hypobaric hypoxia***

226 The complexity of the BF and oxyHb signals arising from oscillatory flow-motion activity was  
227 determined using non-linear LZ complexity (LZC) analysis. Examination of the BF signals  
228 obtained from SH and LL at BL and on ascent to EBC, revealed that the information content  
229 of the BF signals remained relatively constant over the 15 epochs (600s) analysed in both  
230 groups under normoxia and hypobaric hypoxia. As previously, it was thus deemed  
231 appropriate to additionally present the complexity of each signal as a mean LZC index<sup>22,23</sup>.

232 **Fig 2** shows that the complexity of resting BF signals measured at the forearm and finger in  
233 SH and LL remained relatively constant over the 15 epochs sampled, at both BL and EBC.  
234 LZC index (mean LZC of 15 epochs) of the BF signal in both the forearm and finger  
235 microvascular beds was significantly influenced by group (forearm: p=0.0001, F=15.6; finger:  
236 p<0.0001, F=59.9), and site (forearm: p=0.0013, F=10.7; finger p=0.0025, F=9.5). Forearm

237 BF LZC index increased in SH with ascent to EBC (BL vs EBC  $p < 0.0031$ ), and at EBC was  
 238 significantly greater than that of LL (SH vs LL  $p < 0.0001$ ) (**Fig 3**). There was no association  
 239 between forearm BF LZC index and resting BF or skin temperature at BL or EBC in SH or  
 240 LL.

241 LZC index of the finger BF signal was higher in SH than LL at both BL and EBC (both  
 242  $p < 0.0001$ ), but only increased with ascent to EBC in LL ( $p = 0.0413$ ) (**Fig 3**). In SH, finger BF  
 243 LZC index was positively associated with RF ( $p < 0.001$  at both BL and EBC) and skin  
 244 temperature at both altitudes ( $p = 0.001$  at both BL and EBC). No such association was seen  
 245 in LL.

246 Neither age nor sex were independently associated with BF LZC index in SH. However, in  
 247 LL age was negatively associated with forearm BF LZC index ( $r = -0.491$   $p = 0.004$ ).

248 We found no significant difference in LZC index of the oxyHb signals measured at the  
 249 forearm between LL and SH, at either BL or EBC ( $p > 0.05$ ) (**Fig 4**). However, in SH forearm  
 250 BF LZC index was positively associated with the LZC index of the oxyHb signal at both BL  
 251 ( $r = 0.414$   $p = 0.005$ ) and EBC ( $r = 0.307$   $p = 0.004$ ). No such association was found in LL at BL  
 252 ( $p = 0.672$ ), and only approached significance at EBC ( $r = 0.353$   $p = 0.065$ ).

253

#### 254 ***Changes in multiscale LZC (MLZC) at altitude are associated with flow-motion activity***

255 The LZC of the BF signals at the forearm was computed over 12 scales for all LL and SH at  
 256 BL and EBC (**Fig 5**). As the scale length increased, so too did LZC, with better separation  
 257 seen at certain scales. In both SH and LL, the largest differences between the LZC values at  
 258 BL and EBC were for time scales  $> 10$  in both forearm and finger microvascular beds  
 259 ( $p < 0.05$ ).

260 **Fig 6** shows the association of the power in the five spectral bands to LZC forearm and  
 261 finger BF complexity at each scale for the two groups at each altitude. There were clear  
 262 differences in the associations between LZC and spectral power in the five bands both  
 263 between SH and LL, and between BL and EBC in the forearm and finger BF signals. In LL,  
 264 cardiac activity negatively associated with forearm BF LZC at all scales at both altitudes.  
 265 Power in the respiratory band was positively associated with LZC up to scale at BL, but did  
 266 not reach significance at EBC. In the low frequency bands, the myogenic activity negatively  
 267 associated with LZC at EBC over scales  $\tau = 1-12$  (40 - 3.34 Hz sample rate). No significant  
 268 association was found with power in the neurogenic activity band, and LZC at any scale at  
 269 either BL or EBC in LL. In SH, there was no association between LZC and spectral power in  
 270 any band at BL. At EBC, there was a significant negative association between myogenic



271 activity and forearm BF LZC, and a positive association between neurogenic activity and BF  
272 LZC across scales  $\tau = 2-11$ . No association between forearm BF LZC and the high  
273 frequency activity bands was seen at either altitude in SH.

274 Similar trends were seen in the association between spectral power in the five bands and  
275 LZC in the finger BF signals. However, the only associations between BF LZC and spectral  
276 power that reached significance in the finger were in LL at BL, where cardiac activity  
277 negatively associated with BF LZC, and myogenic activity negatively associated with BF  
278 LZC at all scales (**Fig 6**).

279

280

## 281 **DISCUSSION**

282 We have shown that the LZ complexity of the skin microvascular blood flux signals,  
283 measured in participants of the XE2 research expedition<sup>28</sup>, increased with ascent to EBC  
284 (5300m). We observed that SH exhibited a greater level of network complexity and hence  
285 capacity for heterogeneous flow distribution than LL, at both BL and EBC. We also found  
286 clear differences in the influence of local flow-motion activity on the information content, and  
287 hence complexity of the BF signal, between SH and LL on ascent to altitude. Finally, we  
288 have shown that in SH, the increased complexity of microvascular network perfusion is  
289 associated with an enhanced complexity of the simultaneously sampled oxyHb signals,  
290 suggestive of an improved ability in SH to match O<sub>2</sub> demand to local O<sub>2</sub> delivery under  
291 conditions of hypobaric hypoxia.

292

293 We have previously shown using time and spectral domain signal analysis that SH, when  
294 exposed to hypobaric hypoxia, demonstrated superior preservation of peripheral  
295 microcirculatory perfusion compared to LL and that physiological differences in local  
296 microvasculature myogenic (vasomotor) and neurogenic control may play a key role in that  
297 adaptation of SH to high altitude hypobaric hypoxia by sustaining local perfusion and tissue  
298 oxygenation. However, a robust and consistent mechanistic description of flow dynamics  
299 within the microcirculation cannot be achieved using time domain analysis (in either the  
300 resting state or during haemodynamic perturbation) or frequency domain analysis methods  
301 alone<sup>15</sup>.

302

303 Non-linear complexity-based analysis applied to BF signals derived from the peripheral  
304 vasculature has been shown to yield additional, and much deeper, understanding of the loss  
305 of system flexibility and to enhance risk assessment<sup>25,27</sup>. In the current study, LZC index

306 was higher in SH than LL in both forearm and finger BF signals (**Fig 2 and 3**). It also  
307 increased to a greater extent in SH than LL on ascent to altitude. LZC of the BF signal has  
308 previously been shown to decline in individuals with or at risk of CVD<sup>25</sup> and in a primate  
309 model of diabetes<sup>24</sup>. Similarly, Frisbee et al<sup>32</sup>, using chaotic network attractor analysis to  
310 explore the spatial and temporal shift in perfusion distribution at successive arteriolar  
311 bifurcations within skeletal muscle, have shown an imbalanced and temporally stable  
312 distribution of flow through the microvascular network in rodent models of increasing  
313 metabolic and CV disease risk. Our current findings suggest that the increase in capacity  
314 for variability in the BF signal seen in SH is indicative of an enhanced adaptive capacity at  
315 altitude and thus may indicate more effective autoregulation within the microvascular  
316 system<sup>22,33,34</sup>.

317

318 Distributive alterations and heterogeneity of flow within microvascular networks are critical to  
319 an adequate tissue oxygenation<sup>10,11</sup> and oscillatory fluctuations in microvascular network flow  
320 have been shown to ensure a more effective tissue oxygenation than would be obtained with  
321 a steady blood flow<sup>16</sup>. While we report no change in LZC of the oxyHb signal with ascent to  
322 EBC nor differences between SH and LL, we did observe a positive association between the  
323 LZC index of forearm BF and LZC index of oxyHb signals in SH, measured simultaneously  
324 at the forearm, at both BL and EBC. We additionally found that in SH the enhanced  
325 complexity of network perfusion measured at both altitudes was positively associated  
326 ( $r=0.252$   $p=0.019$ ) with the previously reported microvascular oxygen unloading rate,  
327 measured in the same individuals<sup>8</sup>. Such a relationship was not seen in LL ( $p=0.761$ ). The  
328 distribution of O<sub>2</sub> in tissue depends on microvascular network structure and flow and  
329 haematocrit distributions, which are all markedly heterogeneous<sup>10</sup>. Disturbed capillary flow  
330 patterns have been shown to limit the efficacy of oxygen extraction even in the absence of  
331 changes in mean flow<sup>35</sup>. While we are unable to demonstrate a causal relationship between  
332 microvascular blood flow, complexity of the perfusion signals and tissue oxygenation, such a  
333 relationship would appear consistent with a beneficial adaptation in SH whereby enhanced  
334 variability in flow-motion activity gives rise to more effective O<sub>2</sub> unloading.

335

336 The increase in LZC index derived from laser Doppler BF signals from the skin with ascent  
337 to EBC, and the differences in variability of the signals between SH and LL, appear at first to  
338 be contrary to the decrease in flow heterogeneity index (HI) reported by Gilbert-Kawai et al<sup>7</sup>  
339 derived from direct observation of the movement of red blood cells in the buccal mucosal  
340 microcirculatory bed using incident dark-field imaging. In this study of 64 SH and 69 LL from  
341 XE2, Gilbert-Kawai et al report that in SH sublingual blood flow increases on ascent to high  
342 altitude in a "uniform and homogenous manner" in vessels <25  $\mu\text{m}$ . By contrast they report

343 that in LL microvascular flow decreased, but observed that this decrease was “not in a  
344 uniform manner, such that it became heterogeneous in nature”. HI is calculated using a  
345 semi-quantitative technique, as the highest site flow velocity minus the lowest site flow  
346 velocity divided by the mean of the flow velocities across all sublingual vessels imaged<sup>36</sup>. HI  
347 is thus indicative of variations in red blood cell flow velocities across a series of individual  
348 capillaries, while LZC index is a measure of the algorithmic complexity of the time series  
349 data of the laser Doppler blood flux signal and yields a measure of the variability or  
350 predictability of the oscillatory signal. As such, these indices cannot be compared. It should  
351 not be neglected that capillary density has been reported to increase under conditions of  
352 hypobaric hypoxia<sup>1</sup>, and that while Gilbert-Kawai et al<sup>7</sup> report that sublingual small vessel  
353 density was not different between the SH and LL at BL testing, capillary density was up to  
354 30% greater in SH at EBC. Taken together, these data from the buccal mucosa suggest that  
355 SH maintain a significantly greater microcirculatory flow per unit time and flow per unit  
356 volume of tissue than LL at high altitude; an anticipated consequence of which might be  
357 greater information content of the BF signals and consequently a higher LZC.

358

359 From a signal perspective, variability in BF arises from the cumulative activity of all the  
360 processes modulating BF and their temporal variation. Fluctuations in microcirculatory flow  
361 occur at different frequencies related to local endothelial (0.0095-0.02Hz), sympathetic  
362 (0.02-0.06Hz) activity, myogenic activity in the vessel wall (0.06-0.15Hz), and modulation by  
363 respiratory (0.15-0.4Hz), and heart (0.4-1.6Hz) rates<sup>14</sup>. Examination of the information  
364 content of the BF signals from SH and LL revealed a clear and significant difference in LZC  
365 between the two groups on ascent to altitude that becomes more pronounced at certain  
366 timescales (or sampling rates). Furthermore, by examining the association of the individual  
367 spectral bands associated with flow-motion with the different time-scales in MLZC, our data  
368 provide strong evidence that the influence of the modulators of flow-motion activity differs  
369 between SH and LL and with ascent to altitude. The Spearman correlations between the  
370 power bands of the forearm BF signals and LZC across multiple time scales shown in **Fig 6**  
371 showed that in LL there was a significant contribution of cardiac power compared with SH, at  
372 both BL and EBC. Consequently, the BF signal had proportionally more periodic content in  
373 LL and the complexity of the signal was reduced as the information content falls. Previous  
374 studies in altitude-naïve LL and high altitude residents have shown that autonomic function,  
375 heart rate variability and respiration rate are differentially affected at high altitude, with LL  
376 showing sympathetic activation to modulate the direct vasodilatory effects of hypobaric  
377 hypoxia<sup>37,38</sup>. Heart rate variability is also known to contribute to complexity of the BF  
378 signal<sup>39,40</sup> and cardiac rhythm to be modulated by respiratory oscillation<sup>41</sup>. This coupling of

379 the two HF components offers a possible partial explanation as to why the MLZC increases  
380 with scale in both SH and LL (**Fig 5**).

381

382 The lower frequencies associated with flow-motion (that generally contain most of the power  
383 in the signal) also contributed to signal variability. We report a marked uprating of the  
384 association between neurogenic power with LZC of BF measured at the forearm at high  
385 altitude, which is positively associated in SH. This appears consistent with the preservation  
386 of vasoconstrictor response and enhanced neurogenic activity reported in SH at altitude  
387 reported previously<sup>8</sup>. Such changes are indicative of an adaptive modulation of sympatho-  
388 vagal activity through which SH can better regulate flow, allowing them to stay in a hypobaric  
389 atmosphere at lower temperatures without excessive autonomic stress<sup>42</sup>. These adaptations  
390 may also contribute to the higher skin temperatures measured in SH. We saw no significant  
391 uprating of the association between neurogenic power and LZC of BF at any scale  
392 measured at the forearm of LL at high altitude.

393

394 Myogenic activity (vasomotion) is closely associated with effective oxygen delivery<sup>17,43,44</sup> and  
395 has been shown to increase in hypobaric hypoxia<sup>8,9</sup>. Consistent with this we observed an  
396 increased association of the myogenic power band with LZC of the blood flux signal over  
397 multiple time scales in both SH and LL, under conditions of hypobaric hypoxia at EBC. The  
398 association of myogenic power with BF LZC was negative, consistent with its periodic  
399 nature. While the effect of flow-motion on the transport of oxygen to tissue 'is highly  
400 complicated'<sup>45</sup>, an increase in the lower frequencies of flow-motion and particularly in  
401 vasomotion has been shown to give rise to transients in the partial pressure of O<sub>2</sub> (PO<sub>2</sub>) to  
402 substantially increase the volume of oxygenated tissue and to oxygenate tissue domains  
403 which under steady-state conditions would remain anoxic<sup>11</sup>. Indeed, mathematical modelling  
404 suggests that vasomotion activity can change oxygen delivery to tissues by up to eightfold  
405 under certain conditions<sup>46</sup>. Clinically, it has been shown that vasomotion is increased in  
406 patients with mild peripheral arterial occlusive disease (PAOD) and that those patients with  
407 flow-motion had significantly higher tissue oxygen levels than those without, despite similar  
408 blood flow<sup>47</sup>. Our data are also consistent with the increase in vasomotion seen in reduced  
409 perfusion states such as sepsis and cardiopulmonary bypass and in multiple organ  
410 dysfunction and mortality<sup>48-50</sup>. Thus, the increased strength of the association of the  
411 myogenic power band activity with LZC, is consistent with vasomotion being an important  
412 modulator of gaseous exchange under conditions of hypobaric hypoxia, when the  
413 microcirculation may tend towards a critical state.

414

415 We found little association between forearm BF LZC and the power of the endothelial  
416 frequency band in either LL or SH. While the strength of the association in SH was greater at  
417 EBC than at BL, it only reached significance at the highest sampling frequency of 40 Hz ( $r$   
418  $=1$ ). Thus, while endothelium-mediated flow-motion might be expected to enhance network  
419 perfusion and tissue oxygenation, we can as yet draw few conclusions on the role of the  
420 endothelium-attributed flow-motion activity within the skin microvasculature at altitude.

421

422 This study has several strengths, not least the large and sex balanced group size. While we  
423 saw no independent effect of sex or BMI on our outcome measures of complexity in either  
424 SH or LL, we did observe a negative effect of age on BF LZC index in LL but not in SH. LL  
425 (mean age 46(14)y) were significantly older than the SH (28(6)y) ( $p=0.0001$ , SH vs LL) in  
426 this subset of participants from XE2, and it is probable that increasing age constitutes a risk  
427 factor for declining heterogeneity of microcirculatory network perfusion<sup>51</sup>. A similar age-  
428 related reduction in signal complexity has been reported using nonlinear measures applied  
429 to cardiac signals<sup>52</sup> and signals derived from large blood vessel (pulse wave velocity)<sup>53</sup>.

430 To the best of our knowledge, this study is the first to analyse the effect of hypobaric hypoxia  
431 at high altitude on the microcirculation using complexity-based measures applied to skin  
432 microvascular LD blood flux signals. We have previously demonstrated that complexity-  
433 based measures can differentiate both between haemodynamic states<sup>22,23</sup> and between  
434 groups of individuals at increasing risk of developing microvascular dysfunction<sup>25</sup>. The  
435 current study extends and strengthens the utility of these approaches to widely varying  
436 cohorts.

437 We analysed signals from two skin sites that allowed us to explore the differential impact of  
438 local flow-motion activity on network flow heterogeneity. Skin is a major thermoregulatory  
439 organ sensitive to environmental temperature. The temperature of the London laboratory  
440 where baseline measurements were performed in lowlanders was lower than that in  
441 Kathmandu where Sherpas were studied. It is therefore probable that this contributed to the  
442 lower forearm and finger fluxes seen in Lowlanders at baseline. While both cohorts were  
443 exposed to the same laboratory conditions at EBC, finger BF and skin temperature remained  
444 significantly higher in SH than LL. This suggests that the physiological differences in SH and  
445 LL seen at EBC are independent of external temperature. However, the variations in skin  
446 temperature across the cohorts and altitudes may be expected to differentially influence  
447 relative flow-motion activity and signal complexity<sup>23</sup> as will differences in haematocrit that  
448 have been reported previously<sup>5-7</sup> and which may influence the laser Doppler signal<sup>8</sup>.

449 The paucity of significant associations between LZC and spectral power across the five  
450 frequency bands measured at the finger was unexpected, as LZC of the BF signals  
451 measured at both the forearm and the finger were higher in SH than LL and both influenced  
452 by ascent to altitude. It was also unexpected as skin BF at the finger is largely determined  
453 by arteriovenous anastomoses under vasoconstrictor sympathetic control<sup>29</sup> and we have  
454 previously shown that ascent to EBC results in differential changes in vasoconstrictor  
455 responses and in local flow-motion activity in the low frequency bands in the resting blood  
456 flux signals in SH and LL<sup>8</sup>.

457 In exploring the associations between LZC and spectral power of the BF signals, we used  
458 fixed non-overlapping intervals to define the spectral bands as described previously by  
459 Stefanovska and colleagues<sup>14</sup>. It is unlikely that the boundaries of these frequency intervals  
460 remain constant across a cohort of individuals, or for a given individual, under changing  
461 conditions of physiological stress. State-dependent fluctuations in frequency intervals may  
462 thus give rise to different patterns in complexity within, and across, the cohorts studied. It  
463 could be interesting to explore further the impact of time-varying spectral band boundaries  
464 on signal complexity, and how this may inform a mechanistic interpretation of the  
465 heterogeneity of microvascular network perfusion.

466

## 467 **CONCLUSIONS**

468 These data confirm that synchronicity of rhythms in the modulators of microcirculatory blood  
469 flux signals, assessed using non-linear complexity analysis, contributes to the heterogeneity  
470 of microvascular perfusion. They also go some way to describe the changes in the activity of  
471 local and systemic physiological mechanisms that modulate the potentially beneficial  
472 adaptation response seen in SH under conditions of hypobaric hypoxia. Together these data  
473 suggest that peripheral tissues play an important physiological role in the cardiovascular  
474 adaptation to hypoxia, and that this role is better developed in native altitude dwellers than in  
475 lowlanders.

476 In future, it is possible that a combination of time, frequency and complexity analysis will  
477 yield a deeper understanding of the loss of system flexibility that may prevent the  
478 microvascular networks from adapting to an imposed stressor and provide further insight into  
479 the parameters that influence this.

480

481

482

**483 DATA AVAILABILITY STATEMENT**

484

485 Data supporting this study are openly available from the University of Southampton  
486 repository at <https://doi.org/10.5258/SOTON/D1076>.

487

488

**489 ACKNOWLEDGEMENTS**

490

491 Xtreme Everest 2 is a research project coordinated by the Xtreme Everest Oxygen Research  
492 Consortium, collaboration between the UCL Centre for Altitude, Space, and Extreme  
493 Environment Medicine, the Centre for Human Integrative Physiology at the University of  
494 Southampton and the Duke University Medical Centre. We thank the Xtreme Everest 2  
495 Research Group for its contribution (Members of the group were S Abraham, T Adams, W  
496 Anseeuw, R Astin, B Basnyat, O Burdall, J Carroll, A Cobb, J Coppel, O Couppis, J Court, A  
497 Cumpsey, T Davies, S Dhillon, N Diamond, C Dougall, T Geliot, E Gilbert-Kawai, G Gilbert-  
498 Kawai, E Gnaiger, M Grocott, C Haldane, P Hennis, J Horscroft, D Howard, S Jack, B Jarvis,  
499 W Jenner, G Jones, J van der Kaaij, J Kenth, A Kotwica, R Kumar BC, J Lacey, V Laner, D  
500 Levett, D Martin, P Meale, K Mitchell, Z Mahomed, J Moonie, A Murray, M Mythen, P  
501 Mythen, K O'Brien, I. Ruggles-Brice, K Salmon, A Sheperdigian, T Smedley, B Symons, C  
502 Tomlinson, A Vercueil, L Wandrag, S Ward, A Wight, C Wilkinson, S Wythe).

503

**504 COMPETING INTERESTS**

505 MPG serves on the medical advisory board of Sphere Medical Ltd. DSM, MPG and MGM are  
506 directors of Oxygen Control Systems Ltd. MPG, DSM, DZHL, MGM & KM serve on the  
507 board of the Xtreme Everest Oxygen Research Consortium and MPG and KM serve as  
508 trustees of the Xtreme Everest charity.

509

**510 AUTHOR CONTRIBUTION**

511 EGK, MM, DL, KM, DM and MPG were involved in the conception and design of the study.  
512 TD, EGK, KM, DL, SW performed experiments. TD, EGK, DC, MT, AJC and GFC analysed  
513 the data. DC, MT, AJC and GFC interpreted the results. DC, MT, AJC and GFC prepared  
514 the first draft of the manuscript. All authors were involved in the revision of the draft

515 manuscript and have approved the final content. All authors agree to be accountable for all  
516 aspects of the work in ensuring questions relating to the accuracy and integrity of any part of  
517 the work are appropriately investigated and resolved. All persons designated as authors  
518 qualify for authorship, and all those who qualify are listed.

519

## 520 **FUNDING**

521 No grant funding supported this work; financial contributions were provided by the following  
522 organisations: Xtreme Everest 2 was supported by the Royal Free Hospital NHS Trust  
523 Charity, the Special Trustees of University College London Hospital NHS Foundation Trust,  
524 the Southampton University Hospital Charity, the UCL Institute of Sports Exercise and  
525 Health, The London Clinic, University College London, University of Southampton, Duke  
526 University Medical School, the United Kingdom Intensive Care Society, the National Institute  
527 of Academic Anaesthesia, the Rhinology and Laryngology Research Fund, The  
528 Physiological Society, Smiths Medical, Deltex Medical, Atlantic Customer Solutions and the  
529 Xtreme Everest 2 volunteer participants who trekked to Everest Base Camp.

530 Some of this work was undertaken at University College London Hospital - University  
531 College London Biomedical Research Centre, which received a proportion of funding from  
532 the United Kingdom Department of Health's National Institute for Health Research  
533 Biomedical Research Centre's funding scheme. Some of this work was undertaken at  
534 University Hospital Southampton, University of Southampton Respiratory Biomedical  
535 Research Unit, which received a proportion of funding from the United Kingdom Department  
536 of Health's National Institute for Health Research Biomedical Research Units funding  
537 scheme. MPG is part funded by the National Institute of Health Research Senior  
538 Investigator Scheme.

539

540

## 541 **REFERENCES**

542

- 543 1. Gilbert-Kawai E. T., Milledge J. S, Grocott M. P. & , Martin D. S. King of the mountains:  
544 Tibetan and Sherpa physiological adaptations for life at high altitude. *Physiology*  
545 (Bethesda).**29**(6), 388-402 (2014).
- 546 2. Beall, C. M. *et al.* Hemoglobin concentration of high-altitude Tibetans and Bolivian  
547 Aymara. *Am. J. Phys. Anthropol.* **106**(3), 385-400 (1998).



- 548 3. Samaja, M., Veicsteinas, A. & Cerretelli, P. Oxygen affinity of blood in altitude Sherpas. *J*  
549 *Appl. Physiol. Respir. Environ. Exerc. Physiol.* **47**(2), 337-341 (1979).
- 550 4. Wu, T. & Kayser, B. High altitude adaptation in Tibetans. *High. Alt. Med. Biol.* **7**(3), 193-  
551 208 (2006).
- 552 5. Martin, D. S. *et al.* Changes in sublingual microcirculatory flow index and vessel density  
553 on ascent to altitude. *Exp. Physiol.* **95**, 880-891 (2010).
- 554 6. Martin, D. S. *et al.* The use of skeletal muscle near infrared spectroscopy and a vascular  
555 occlusion test at high altitude. *High Alt. Med. Biol.* **14**(3), 256–262 (2013).
- 556 7. Gilbert-Kawai, E. *et al.* Sublingual microcirculatory blood flow and vessel density in  
557 Sherpas at high altitude. *J. Appl. Physiol.* (1985) **122**, 1011-1018 (2017).
- 558 8. Davies, T. *et al.* Sustained vasomotor control of skin microcirculation in Sherpas versus  
559 altitude-naive lowlanders: Experimental evidence from Xtreme Everest 2. *Exp. Physiol.*  
560 **103**(11), 1494-1504 (2018).
- 561 9. Salvi, P. *et al.* Increase in slow-wave vasomotion by hypoxia and ischemia in lowlanders  
562 and highlanders. *J. Appl. Physiol.* (1985) **125**(3), 780-789 (2018).
- 563 10. Duling, B. R. & Damon, D. H. An examination of the measurement of flow heterogeneity  
564 in striated muscle. *Circ. Res.* **60**(1), 1-13 (1987).
- 565 11. Tsai, A. G. & Intaglietta, M. Evidence of flowmotion induced changes in local tissue  
566 oxygenation. *Int. J. Microcirc. Clin. Exp.* **12**(1):75-88 (1993).
- 567 12. Segal, S.S. Regulation of blood flow in the microcirculation. *Microcirculation.* **12**, 33–45.  
568 (2005).
- 569 13. Rossi, M., Carpi A., Galetta, F., Franzoni, F, Santoro, G. The investigation of skin blood  
570 flowmotion: a new approach to study the microcirculatory impairment in vascular  
571 diseases? *Biomed Pharmacother.* **60**, 437– 442 (2006).
- 572 14. Kvandal, P. *et al.* Low-frequency oscillations of the laser Doppler perfusion signal in  
573 human skin. *Microvasc. Res.* **72**, 120-127 (2006).
- 574 15. Clough, G. F., Kuliga, K. Z. & Chipperfield, A. J. Flow motion dynamics of microvascular  
575 blood flow and oxygenation: Evidence of adaptive changes in obesity and type 2  
576 diabetes mellitus/insulin resistance. *Microcirculation* **24**(2) e12331 (2017).
- 577 16. Nilsson, H. & Aalkjaer, C. Vasomotion: mechanisms and physiological importance. *Mol.*  
578 *Interv.* **3**, 79-89, 51, (2003).
- 579 17. Thorn, C. E., Kyte, H., Slaff, D. W. & Shore, A. C. An association between vasomotion  
580 and oxygen extraction. *Am. J. Physiol. Heart Circ. Physiol.* **301**(2):H442-449, (2011).
- 581 18. Kalev, K., Bachmann, M., Orgo, L., Lass, J., Hinrikus, H. Lempel-Ziv and Multiscale  
582 Lempel-Ziv Complexity in Depression. 37th Annual International Conference of the IEEE  
583 Engineering in Medicine and Biology Society. *IEEE Engineering in Medicine and Biology*  
584 *Society Conference Proceedings*, 4158-4161 (2015).

- 585 19. Valenza, G., Citi, L., Garcia, R. G., Noggle Taylor, J., Toschi, N. & Barbieri, R.  
586 Complexity Variability Assessment of Nonlinear Time-Varying Cardiovascular Control.  
587 *Sci Rep.* **7**, 42779 (2017).
- 588 20. Aboy, M., Hornero, R., Abasolo, D. & Alvarez, D. Interpretation of the Lempel-Ziv  
589 complexity measure in the context of biomedical signal analysis. *IEEE Trans. Biomed.*  
590 *Eng.* **53**, 2282–2288 (2006).
- 591 21. Lempel, A. & Ziv, J. On the complexity of finite sequences. *IEEE Trans. Information*  
592 *Theory.* **22**, 75–81 (1976).
- 593 22. Kuliga, K. Z., Gush, R., Clough, G. F. & Chipperfield, A. J. Time-dependent behavior of  
594 microvascular blood flow and oxygenation: a predictor of functional outcomes. *IEEE*  
595 *Trans. Biomed. Eng.* **65**, 1049–1056, (2018).
- 596 23. Thanaj, M., Chipperfield, A. J. & Clough, G.F. Analysis of microvascular blood flow and  
597 oxygenation: Discrimination between two haemodynamic steady states using nonlinear  
598 measures and multiscale analysis. *Comput. Biol. Med.* **102**, 157–167, (2018).
- 599 24. Tigno, X. T., Hansen, B. C., Nawang, S., Shamekh, R. & Albano, A. M. Vasomotion  
600 becomes less random as diabetes progresses in monkeys. *Microcirculation* **18**, 429–439,  
601 (2011).
- 602 25. Chipperfield, A. J., Thanaj, M., Scorletti, E., Byrne, C. D. & Clough, G.F. Multi-domain  
603 analysis of microvascular flow motion dynamics in NAFLD. *Microcirculation* **25**, e12538,  
604 (2019).
- 605 26. Cerutti, S., Hoyer D, Voss, A. Multiscale, multiorgan and multivariate complexity  
606 analyses of cardiovascular regulation. *Philos. Trans. A Math. Phys. Eng. Sci.* **13**, 1337-  
607 58 (2009).
- 608 27. Humeau, A., Buard, B., Mahe, G., Rousseau, D., Chapeau-Blondeau, F. & Abraham, P.  
609 Multiscale entropy of laser Doppler flowmetry signals in healthy human subjects. *Medical*  
610 *Physics* **37**(12), 6142-6146 (2010).
- 611 28. Gilbert-Kawai, E. *et al.* Design and conduct of Xtreme Everest 2: An observational cohort  
612 study of Sherpa and lowlander responses to graduated hypobaric hypoxia. *F1000 Res.*  
613 **4**, 90 (2015).
- 614 29. Braverman, I. M. The Cutaneous Microcirculation. *J. Invest. Dermatol.* **5**(1), 3–9. (2000).
- 615 30. Liu, L. & Miao, S. The complexity of binary sequences using logistic chaotic maps.  
616 *Complexity.* **21**, 121–129 (2016).
- 617 31. Hu, J., Gao, J. & Principe, J.C. Analysis of Biomedical Signals by the Lempel-Ziv  
618 Complexity: the Effect of Finite Data Size, *IEEE TMBE* **53**(12), 2606-2609 (2016).
- 619 32. Costa, M., Goldberger, A. L. & Peng, C. K. Multiscale entropy analysis of biological  
620 signals. *Phys. Rev. E. Stat. Nonlin. Soft Matter Phys.* **71**(2 Pt 1):021906 (2005).

- 621 33. Frisbee, J. C., Goodwill, A. G., Frisbee, S. J., Butcher, T. J., Wu, F. & Chantler, P. D.  
622 Microvascular perfusion heterogeneity contributes to peripheral vascular disease in  
623 metabolic syndrome: metabolic syndrome and microvascular perfusion. *J. Physiol.* **594**,  
624 2233–2243 (2016).
- 625 34. Gryglewska, B. *et al.* Fractal dimensions of skin microcirculation flow in subjects with  
626 familial predisposition or newly diagnosed hypertension. *Cardiol J.* **18**, 26–32 (2011).
- 627 35. Lücker, A., Secomb, T. W., Weber, B. & Jenny, P. The relation between capillary transit  
628 times and hemoglobin saturation heterogeneity. Part 2: Capillary Networks. *Front.*  
629 *Physiol.* **9**, 1296 (2018).
- 630 36. Trzeciak, S., & Rivers, E. P. Clinical manifestations of disordered microcirculatory  
631 perfusion in severe sepsis. *Crit Care.* **9** Suppl 4, S20-26 (2005).
- 632 37. Hansen, J. & Sander, M. Sympathetic neural overactivity in healthy humans after  
633 prolonged exposure to hypobaric hypoxia. *J. Physiol.* **546**(Pt 3), 921-9219 (2003).
- 634 38. Rostrup, M. Catecholamines, hypoxia and high altitude. *Acta Physiol. Scand.* **162**(3),  
635 389–399 (1998).
- 636 39. Sassi, R., Cerutti, S., Lombardi, F., Malik, M. & Huikuri, H. V. Advances in heart rate  
637 variability signal analysis: joint position statement by the e-Cardiology ESC Working  
638 Group and the European Heart Rhythm Association co-endorsed by the Asia Pacific  
639 Heart Rhythm Society. *Europace.* **17**, 1341–1353 (2015).
- 640 40. Wang, G., Jia, S., Li, H., Wang, Z. & Zhang, W. Exploring the relationship between blood  
641 flux signals and HRV following different thermal stimulations using complexity analysis.  
642 *Sci. Rep.* **8**, 8982 (2018).
- 643 41. Simms, A.E., Paton, J. F. R., Allen, A.M. & Pickering, A.E. Is augmented central  
644 respiratory–sympathetic coupling involved in the generation of hypertension? *Resp.*  
645 *Physiol. Neurobiol.* **174**, 89–97 (2010).
- 646 42. Passino, C. *et al.* Autonomic regulation of heart rate and peripheral circulation:  
647 comparison of high altitude and sea level residents. *Clin. Sci.* **91**, Suppl, 81–83 (1996).
- 648 43. Bertuglia, S., Colantuoni, A., Coppini, G. & Intaglietta, M. Hypoxia- or hyperoxia induced  
649 changes in arteriolar vasomotion in skeletal muscle microcirculation. *Am. J. Physiol.* **260**,  
650 H362-372 (1991).
- 651 44. Schmidt, J. A, Borgstrom, P. & Intaglietta, M. The vascular origin of slow wave  
652 flowmotion in skeletal muscle during local hypotension. *Int. J. Microcirc. Clin. Exp.* **12**,  
653 287- 297 (1993a).
- 654 45. Aalkjær, C., Boedtkjer, D. & Matchkov, V. Vasomotion - what is currently thought? *Acta*  
655 *Physiol (Oxf).* **202**(3), 253-269 (2011).
- 656 46. Kislukhin, V. V. Stochasticity of flow through microcirculation as a regulator of oxygen  
657 delivery. *Theor. Biol. Med. Model.* **7**, 29 (2010).

- 658 47. Schmidt, J. A., Borgstrom, P., Firestone, G. P., von Wichert, P., Intaglietta, M. & Fronek,  
659 A. Periodic hemodynamics (flow motion) in peripheral arterial occlusive disease. *J. Vasc.*  
660 *Surg.* **18**, 207–215 (1993b).
- 661 48. Young, J. D & Cameron, E. M. Dynamics of skin blood flow in human sepsis. *Int. Care*  
662 *Med.* **21**(8), 669–74 (1995).
- 663 49. Podgoreanu, M. V., Stout, R. G., El-Moalem, H. E. & Silverman, D. G. Synchronous  
664 rhythmical vasomotion in the human cutaneous microvasculature during nonpulsatile  
665 cardiopulmonary bypass. *Anesthesiol.* **97**(5), 1110–1117, (2002).
- 666 50. Knotzer, H. *et al.* Oscillation frequency of skin microvascular blood flow is associated  
667 with mortality in critically ill patients. *Acta. Anaesthesiol. Scand.* **51**(6), 701–707 (2007).
- 668 51. Khalil A., Humeau-Heurtier A., Gascoin, L., Abraham, P. & Mahé, G. Aging effect on  
669 microcirculation: A multiscale entropy approach on laser speckle contrast images. *Med.*  
670 *Phys.* **43**(7), 4008 (2016).
- 671 52. Costa, M. & Healey, J. A. Multiscale entropy analysis of complex heart rate dynamics:  
672 discrimination of age and heart failure effects. *Comput. Cardiol.* **30**, 705–708 (2003).
- 673 53. Wu, H. T. *et al.* Multiscale entropy analysis of pulse wave velocity for assessing  
674 atherosclerosis in the aged and diabetic. *IEEE Trans. Biomed. Eng.* **58**(10), 2978–2981  
675 (2011).
- 676

677 **TABLES**

678

679 **Table 1.** Summary of peripheral oxygen saturation (SpO<sub>2</sub>) and skin blood flux and  
 680 oxygenation recorded in the time domain at the forearm and finger in lowlanders (LL) and  
 681 Sherpa highlanders (SH) at baseline (BL) and Everest base camp (EBC, 5300 m). Data are  
 682 median (95% confidence interval) from n=32 LL and n=46 SH. \* BL vs EBC within group, †  
 683 LL vs SH within site. SpO<sub>2</sub> (%) = peripheral oxygen saturation (%) (Nonin Onyx 9500, Nonin  
 684 Medical Inc, Minnesota, USA); Skin BF (PU), = resting laser Doppler skin blood flux  
 685 (perfusion units); StO<sub>2</sub> (%) = tissue oxygen saturation (%); oxyHb (AU) = oxygenated  
 686 haemoglobin (arbitrary units); Skin Temp (°C) = skin temperature (°C) (moorVMS-OXY,  
 687 Moor Instruments Ltd, Axminster, UK).

688

Median (95%CI)	Lowlanders N=32		Sherpa Highlanders N=46	
	BL	EBC	BL	EBC
SpO <sub>2</sub> (%)	98.0(98,99)	77.5*(74,81)	97.2(97,98)	79.1*(78,80)
Skin BF forearm (PU)	11.5(9.1,14.4)	14.1(12.4,15.7)	15.2†(13.2,19.2)	11.2*†(9.2,13.1)
StO <sub>2</sub> forearm (%)	40.9(37.0,45.7)	27.1*(24.4,32.0)	36.3†(34.2,38.2)	28.4*(24.5,30.8)
oxyHb forearm (AU)	6.5(5.6,8.9)	5.9(4.6,8.3)	8.7†(7.3,10.6)	7.2*(5.8,8.7)
Skin BF finger (PU)	46(26,84)	34(21,52)	283†(247,327)	232† (178,278)
Skin Temp forearm (°C)	27.6(26.8,28.2)	28.5(27.6,29.5)	31.4†(30.6,32.7)	28.2*(27.2,30.7)
Skin Temp finger (°C)	23.9(22.7,25.7)	23.7(19.6,25.3)	32.0† (30.0,33.1)	28.2*†(23.6,30.5)

689

690

691 **FIGURE LEGENDS**

692

693 **Figure 1.** Examples of (A) skin BF and oxyHb signals from the forearm and (B) skin BF  
 694 signals from finger measured in the time domain of an individual lowlander and Sherpa  
 695 highlander at baseline (BL, black) and Everest base camp (EBC, 5300 m, blue).

696

697 **Figure 2.** Lempel-Ziv complexity (LZC) of skin BF signal measured over 15 epochs at the  
 698 finger and forearm at baseline (BL, black) and Everest base camp (EBC, 5300 m, blue).  
 699 Mean data ( $\pm$ SEM) are shown as solid lines for n=32 lowlanders and n=46 Sherpa  
 700 highlanders. Significant difference between groups, \*p<0.05, +p<0.001

701

702 **Figure 3.** Lempel-Ziv complexity (LZC) index of skin BF signals measured at the forearm  
 703 and finger in n=32 lowlanders and n=46 Sherpa highlanders at baseline (BL, black) and  
 704 Everest base camp (EBC, 5300 m, blue). Data are median and 95%CI. LZC index (mean  
 705 LZC of 15 epochs) of the BF signal in both the forearm and finger microvascular beds was  
 706 significantly influenced by group (forearm: p=0.0001, F=15.6; finger: p<0.0001, F=59.9), and  
 707 site (forearm: p=0.0013, F=10.7; finger p=0.0025, F=9.5). ns not significant, \*p =0.0003 ,  
 708 \*\*p<0.0001

709

710 **Figure 4.** Lempel-Ziv complexity (LZC) index of skin oxyHb signals measured at the forearm  
 711 in n=32 lowlanders and n=46 Sherpa highlanders at baseline (BL, black) and Everest base  
 712 camp (EBC, 5300 m, blue). Data are median and 95%CI. There was no significant difference  
 713 between groups.

714

715 **Figure 5.** Multiscale Lempel-Ziv complexity (MLZC) measured between scales  $\tau = 1-12$  of  
 716 skin BF signal at baseline (BL, black) and Everest base camp (EBC, 5300 m, blue).at the  
 717 forearm and finger at baseline (BL, black) and Everest base camp (EBC, 5300 m, blue).  
 718 Data are mean  $\pm$  SEM of n=32 lowlanders and n=46 Sherpa highlanders. Significant  
 719 difference between groups, \*p<0.05, +p<0.001

720

721 **Figure 6.** Spearman correlations between the flow-motion spectral power bands  
 722 corresponding to endothelial (0.0095-0.02Hz) (black), neurogenic (0.02-0.06Hz) (green),

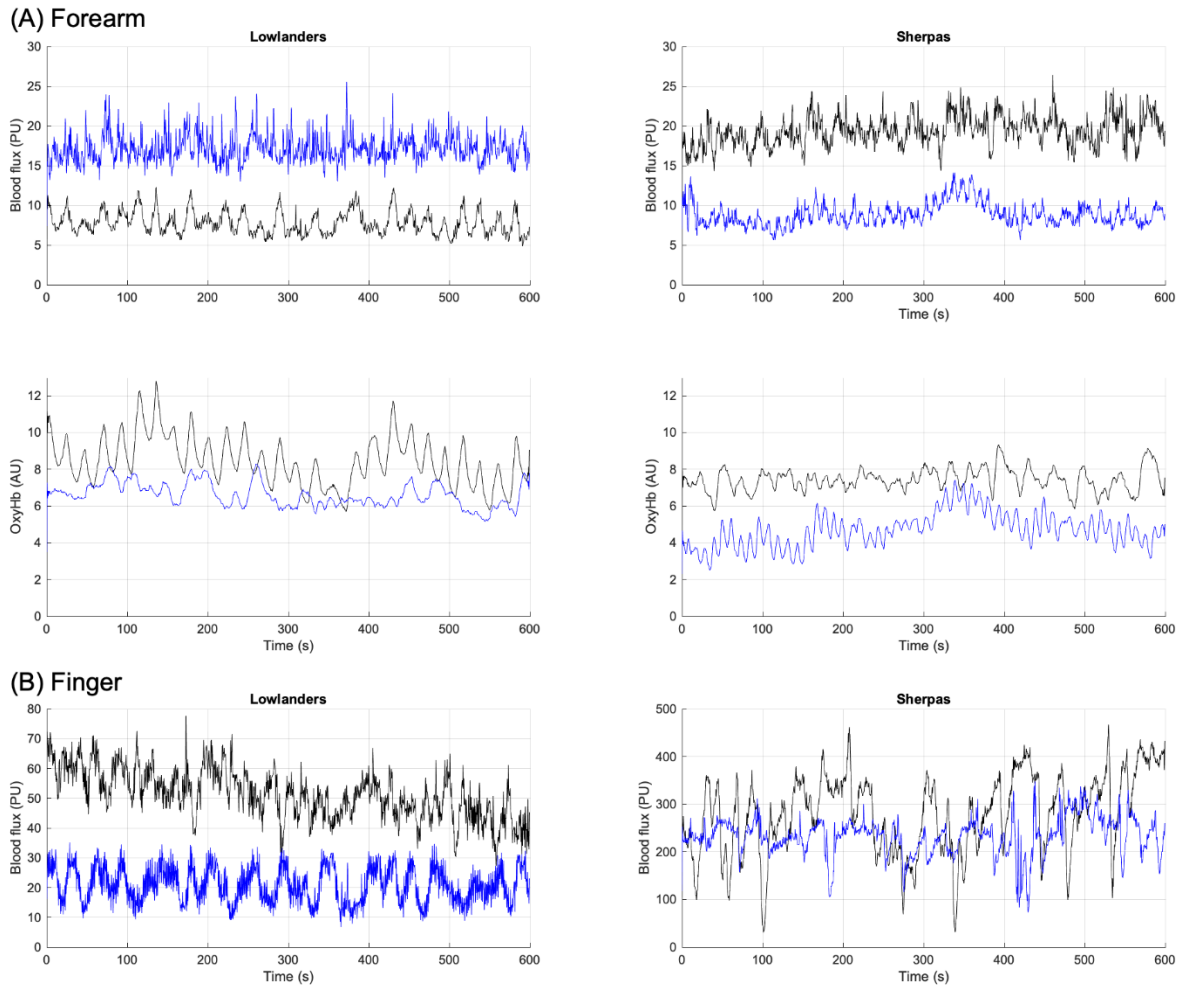
723 myogenic (0.06-0.15Hz) (purple), respiratory (0.15-0.4Hz) (blue), and cardiac (0.4-1.6Hz)  
724 (red) activity and multiscale Lempel-Ziv complexity (MLZC) of the (A) forearm and (B) finger  
725 skin blood flow signals in n=32 lowlanders and n=46 Sherpa highlanders at baseline (BL)  
726 and Everest base camp (EBC, 5300 m). Effective sampling rate = 40Hz/scale. \*p<0.05  
727 +p<0.01.

728 **FIGURES**

729

730 **Figure 1.** Examples of (A) skin BF and oxyHb signals from the forearm and (B) skin BF  
 731 signals from finger measured in the time domain of an individual lowlander and Sherpa  
 732 highlander at baseline (BL, black) and Everest base camp (EBC, 5300 m, blue).

733

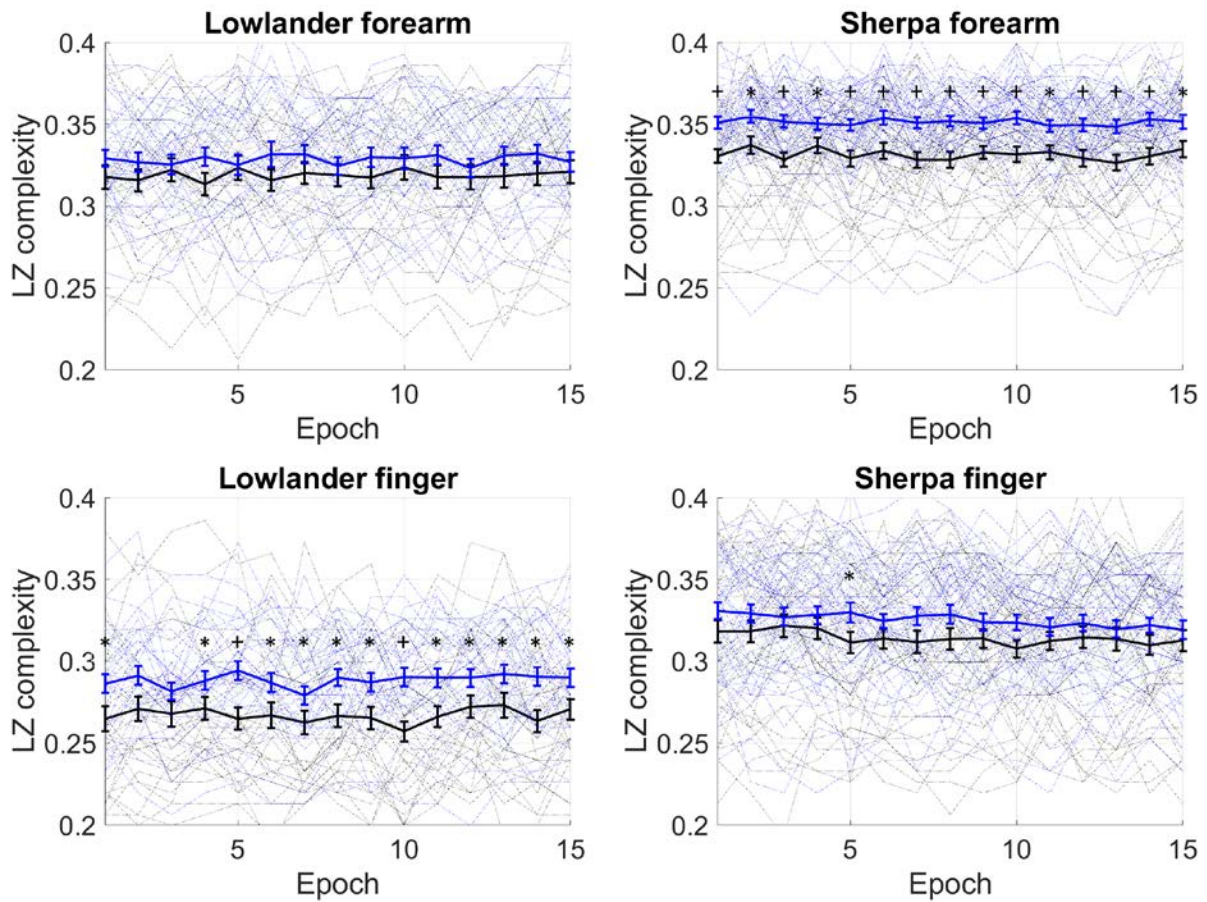


734



735 **Figure 2.** Lempel-Ziv complexity (LZC) of skin BF signal measured over 15 epochs at the  
 736 forearm and finger at baseline (BL, black) and Everest base camp (EBC, 5300 m, blue).  
 737 Mean data ( $\pm$ SEM) are shown as solid lines for  $n=32$  lowlanders and  $n=46$  Sherpa  
 738 highlanders. Significant difference between groups, \* $p<0.05$ , + $p<0.001$

739



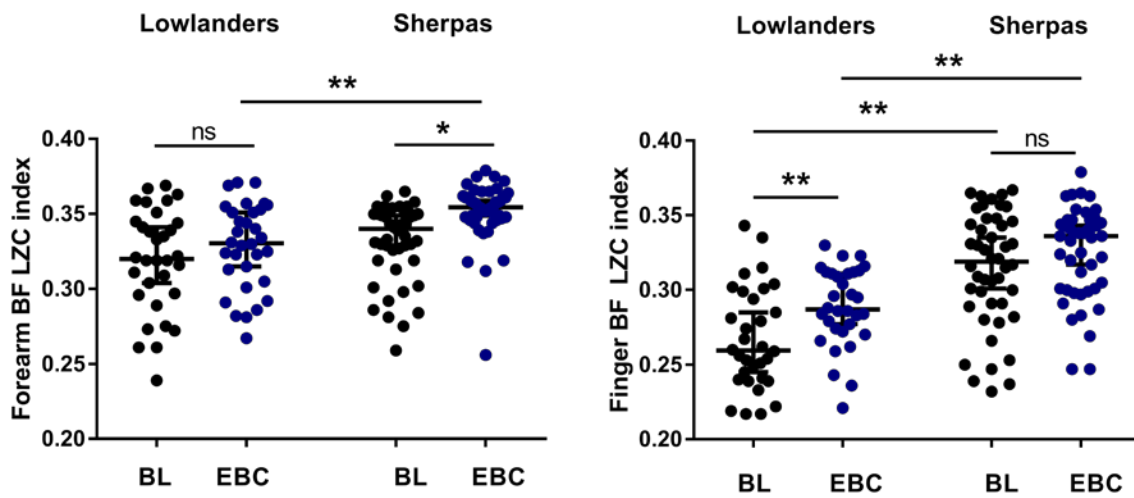
740

741

742

743 **Figure 3.** Lempel-Ziv complexity (LZC) index of skin BF signals measured at the forearm  
 744 and finger in n=32 lowlanders and n=46 Sherpa highlanders at baseline (BL, black) and  
 745 Everest base camp (EBC, 5300 m, blue). Data are median and 95%CI. LZC index (mean  
 746 LZC of 15 epochs) of the BF signal in both the forearm and finger microvascular beds was  
 747 significantly influenced by group (forearm:  $p=0.0001$ ,  $F=15.6$ ; finger:  $p<0.0001$ ,  $F=59.9$ ), and  
 748 site (forearm:  $p=0.0013$ ,  $F=10.7$ ; finger  $p=0.0025$ ,  $F=9.5$ ). ns not significant, \* $p=0.0003$  ,  
 749 \*\* $p<0.0001$

750



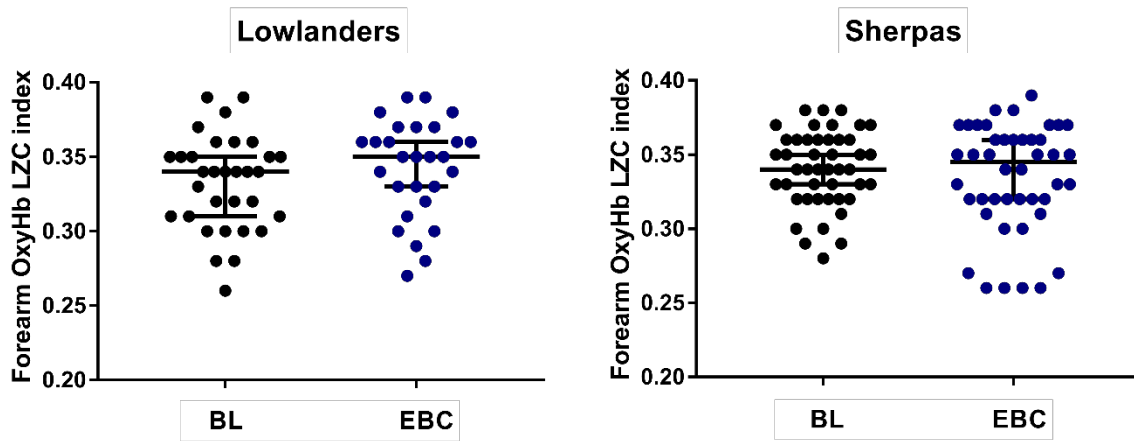
751

752

753 **Figure 4.** Lempel-Ziv complexity (LZC) index of skin oxyHb signals measured at the forearm  
754 in n=32 lowlanders and n=46 Sherpa highlanders at baseline (BL, black) and Everest base  
755 camp (EBC, 5300 m, blue). Data are median and 95%CI. There was no significant difference  
756 between groups.

757

758



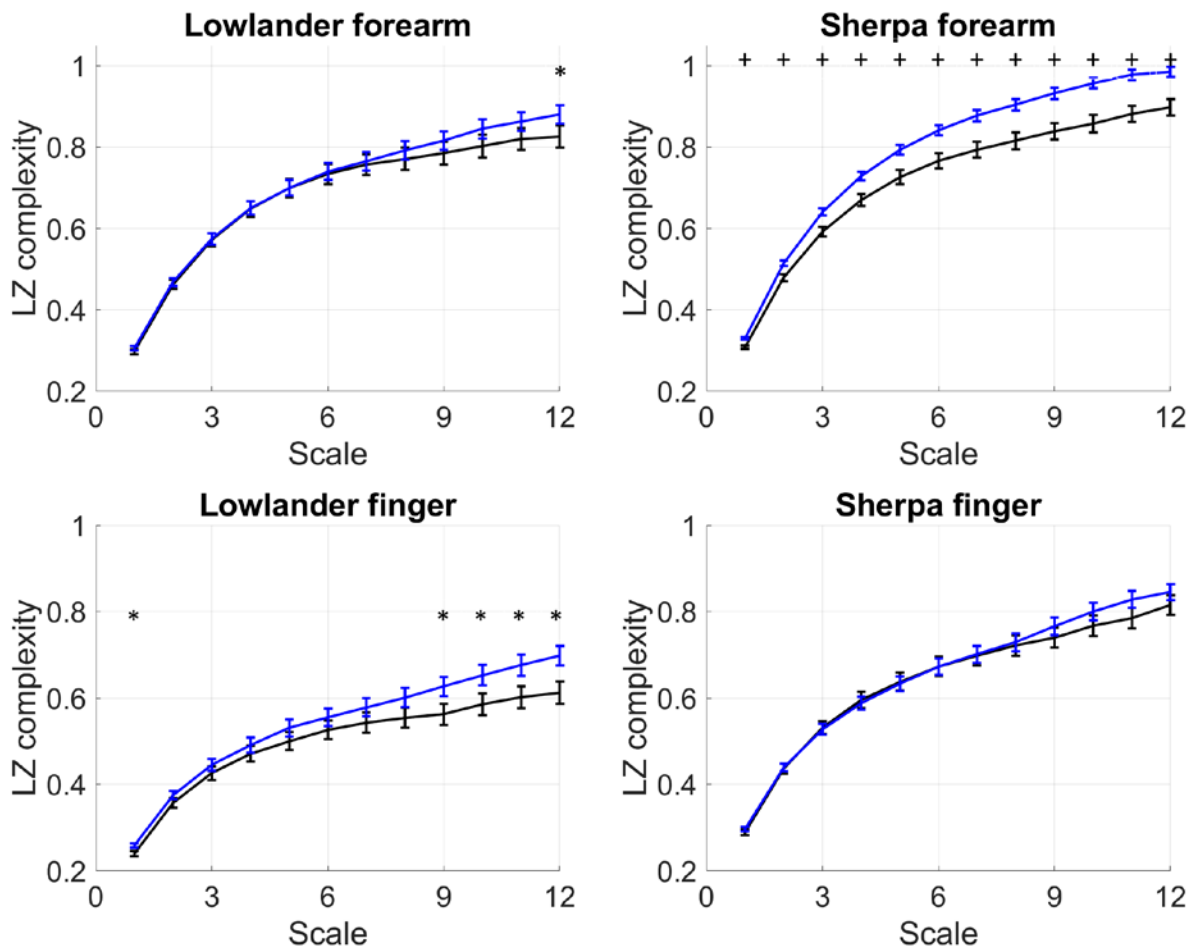
759

760

761 **Figure 5.** Multiscale Lempel-Ziv complexity (MLZC) measured between scales  $\tau = 1-12$  of  
 762 skin BF signal at baseline (BL, black) and Everest base camp (EBC, 5300 m, blue) at the  
 763 forearm and finger at baseline (BL, black) and Everest base camp (EBC, 5300 m, blue).  
 764 Data are mean  $\pm$  SEM of  $n=32$  lowlanders and  $n=46$  Sherpa highlanders. Significant  
 765 difference between groups, \* $p<0.05$ , + $p<0.001$

766

767



768

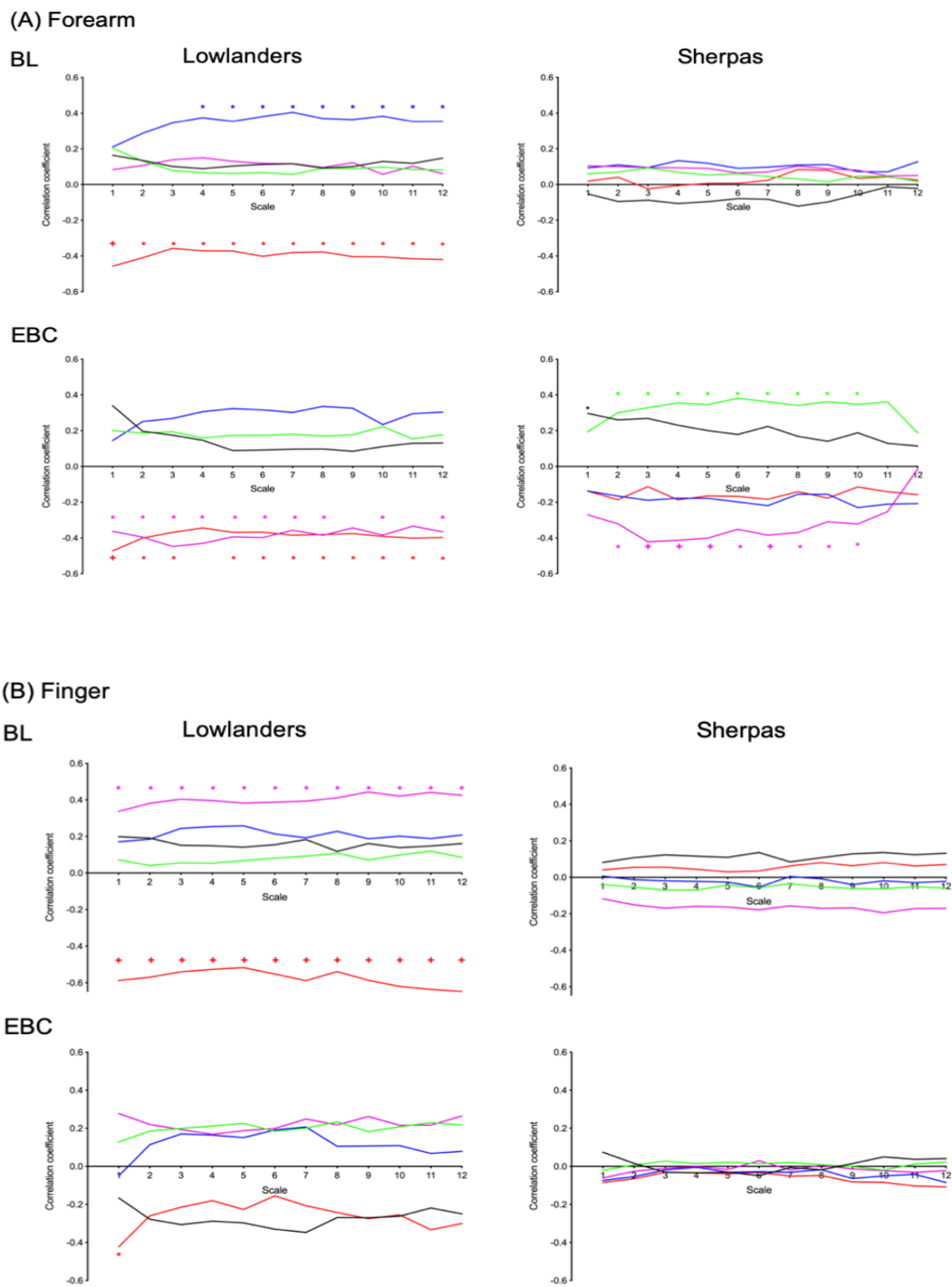
769

770

771

772 **Figure 6.** Spearman correlations between the flow-motion spectral power bands  
 773 corresponding to endothelial (0.0095-0.02Hz) (black), neurogenic (0.02-0.06Hz) (green),  
 774 myogenic (0.06-0.15Hz) (purple), respiratory (0.15-0.4Hz) (blue), and cardiac (0.4-1.6Hz)  
 775 (red) activity and multiscale Lempel-Ziv complexity (MLZC) of the (A) forearm and (B) finger  
 776 skin blood flow signals in n=32 Lowlanders and n=46 Sherpa highlanders at baseline (BL)  
 777 and Everest base camp (EBC, 5300 m). Effective sampling rate = 40Hz/scale. \*p<0.05  
 778 +p<0.01.

779



780

781

782